

Positron annihilation study of η' precipitation kinetics in an aluminium alloy

This article has been downloaded from IOPscience. Please scroll down to see the full text article.

1989 J. Phys.: Condens. Matter 1 3679

(<http://iopscience.iop.org/0953-8984/1/23/012>)

View [the table of contents for this issue](#), or go to the [journal homepage](#) for more

Download details:

IP Address: 171.66.16.93

The article was downloaded on 10/05/2010 at 18:17

Please note that [terms and conditions apply](#).

Positron annihilation study of η' precipitation kinetics in an aluminium alloy

S Abis†, M Biasini‡, A Dupasquier§, P Sferlazzo‡ and A Somoza§||

† Federal Mogul SpA, Via Trione 5, 10081 Cuorgné TO, Italy

‡ ENEA, Dipartimento TIB, Via Mazzini 2, 40137 Bologna BO, Italy

§ Istituto di Fisica del Politecnico, Piazza L da Vinci 32, 20133 Milano MI, Italy

|| Universidad Nac. del Centro de la Pcia. de Buenos Aires, Pinto 399, 7000 Tandil, República Argentina

Received 2 September 1988, in final form 15 November 1988

Abstract. The decomposition of a technical Al-based alloy (Zergal 4) has been studied by positron annihilation techniques. The observed dependence of annihilation characteristics on the aging time is attributed to a change in the positron state due to the transformation of Guinier–Preston zones into semi-coherent η' particles. Predictions based on the Lifshitz–Slyozov–Wagner precipitation theory are in excellent agreement with the experimental data.

1. Introduction

After the pioneering work of Sedov *et al* (1970), the sensitivity of positron annihilation characteristics to precipitation phenomena occurring in aluminium alloys has been firmly established in a number of experiments (for a recent review, see Krause *et al* (1987)). In particular, systematic studies of binary and ternary systems mostly by the Halle group (Dlubek 1984, Dlubek *et al* 1979, 1981a, b, 1983, 1985, 1986, Kabisch *et al* 1980, Alam and West 1982) have convincingly elucidated the role played by the precipitates and associated lattice defects in determining the state, and thus the annihilation characteristics, of positrons in supersaturated alloys at different stages of decomposition.

Thus, the time could be ripe for using positron annihilation in the study of metallurgical problems. The crucial step that has still to be taken in this field, in order to make positron annihilation as effective as small-angle x-ray and neutron scattering (SAXS and SANS) for the structural analysis of alloys, is to work out mathematical models enabling us to convert annihilation data to direct information on the size distribution and on the formation kinetics of precipitates. After almost two decades of positron experiments on aluminium alloys, very little progress has been made in this direction. However, in the present work we discuss a fortunate but important case for which the equations that link annihilation characteristics with the size distribution of precipitates can be derived from the well known positron trapping model. This gives us the possibility to show, in the specific case of an age-hardenable alloy, that the experimental dependence of annihilation characteristics on the aging time is in strict agreement with predictions based on the Lifshitz–Slyozov–Wagner (LSW) theory of precipitation kinetics (Lifshitz and Slyozov 1959, 1961, Wagner 1961).

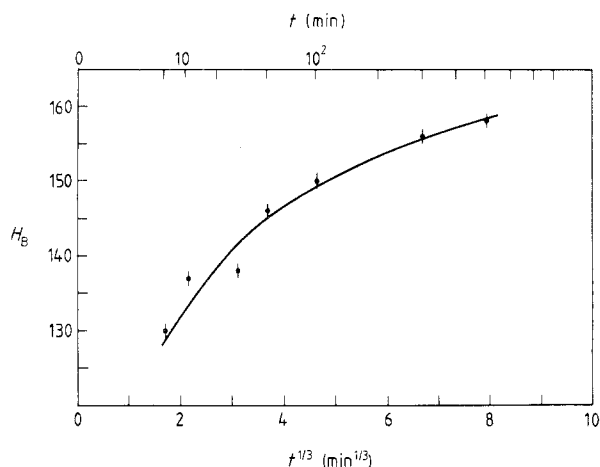


Figure 1. Brinell hardness of the 7012 alloy versus aging time. The curve through the experimental points is a graphic interpolation.

An important point of our work is that our experiments concern a commercial alloy containing inclusions and stable precipitates, which can trap positrons and, in principle, might offset the effect of structural transformations on positron annihilation. On the contrary, not only do we confirm the encouraging but sparse evidence gathered so far for other technical systems (Johnson *et al* 1977, Wang and Wang 1982, Triftshäuser and Kögel 1985), which indicates that the satisfactory sensitivity of the technique is not limited to binary and ternary alloys prepared in controlled laboratory conditions, but we also extend the interpretation scheme proposed by the Halle group to a more complicated situation.

2. Experimental details

We have examined a series of samples in the form of discs (10 mm diameter \times 1 mm thick), cut from a rod of 7012 aluminium alloy (commercial name Zergal 4). The nominal composition (in atomic per cent) of this alloy is: Zn 6.0%, Mg 2.0%, Cu 1.0%, Zr 0.12%, Mn 0.10%, Ti 0.06%, Fe <0.25%, Si <0.15%, Cr <0.04%, Al to balance; detailed information on other properties is given in Di Russo and Buratti (1979).

We have prepared our samples by a typical two-stage aging treatment as follows: (a) solubilisation at 470 °C for 2 h; (b) water quenching at 20 °C; (c) pre-aging at 20 °C for 5 days; (d) aging at 160 °C for different times up to 500 min; (e) water quenching at 20 °C at the end of each aging period. All subsequent manipulations and measurements were performed at room temperature.

The Brinell hardness of the aged samples was measured with a conventional testing machine. The results are reported in figure 1; we have used a non-linear scale for the aging time axis in this and following figures not only for a better presentation of the data, but also for theoretical reasons to be discussed in § 3, which indicate that the alloy evolution follows a $t^{1/3}$ law. The figure shows that the hardness increases with the aging time with no evident indication of an incubation period, and continues to increase till the end of the explored time interval, without signs of over-aging. Almost 60% of the total increase occurs within the first 50 min.

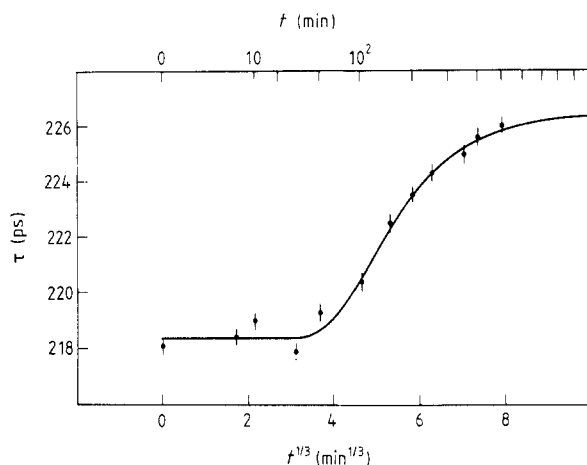


Figure 2. Mean life of positrons annihilated in the 7012 alloy versus aging time. The curve is calculated according to the model discussed in the text.

TEM micrographs were taken with magnification of 10^5 for solubilised and for 500 min aged samples; besides large inclusions present in both cases, a fine and dense granular structure, due to precipitates of sizes below 10 nm, is discernible in the aged material.

Positron annihilation measurements were performed using the standard positron source-sample sandwich geometry; the source (ca 4×10^5 Bq of ^{22}Na from NaCl solution) was deposited onto a mica foil of surface density 1.1 mg cm^{-2} and covered with an identical foil. With this arrangement, the fraction of annihilation occurring in mica, evaluated according to Bertolaccini and Zappa (1967), is 4.8%. Lifetime measurements were performed with a conventional apparatus giving a resolution of 290 ps (full width at half-maximum of the prompt curve). At least three different spectra, with around 10^6 coincidences in each spectrum, were taken for each sample. The spectra were analysed in two components plus the source contribution by means of the EXTENDED POSITRONFIT routine (Kirkegaard and Eldrup 1974, Kirkegaard *et al* 1981). The model always fitted the data well (chi-square/degrees of freedom close to 1.0), but the results for the intensities and the lifetimes of the two components displayed fluctuations larger than the pure statistical indetermination. This inconvenience may occur when the lifetimes to be resolved are too close, or when the intensity of one component is too small. Fortunately, if one takes the results of the analysis for calculating the mean life τ (weighted average of the two lifetimes), most of the erratic fluctuations cancel; in our case, τ turns out to be reproducible within 0.3 ps. For this reason, we present below the results of our measurements in terms of τ ; this form of presentation is adopted very frequently in papers concerning annihilation in metal alloys.

The experimental points are reported in figure 2. As already observed for ternary aluminium alloys with Zn and Mg (Dlubek *et al* 1981a, b, 1983, 1986), the mean life turns out to be larger than in pure Al (our set-up gives $\tau = 162$ ps for annealed Al) even at the earliest stages of aging; after an initial incubation period of ca 50 min (the best fit with a theoretical expression discussed below gives 45 ± 5 min), τ increases monotonically with the aging time, reaching at 500 min a total variation of ca 8 ps, almost 30 times larger than the reproducibility limit of a single experimental point. A stage of decreasing lifetimes, as observed by Triftshäuser and Kögel (1985) for long agings, was not reached in our case.

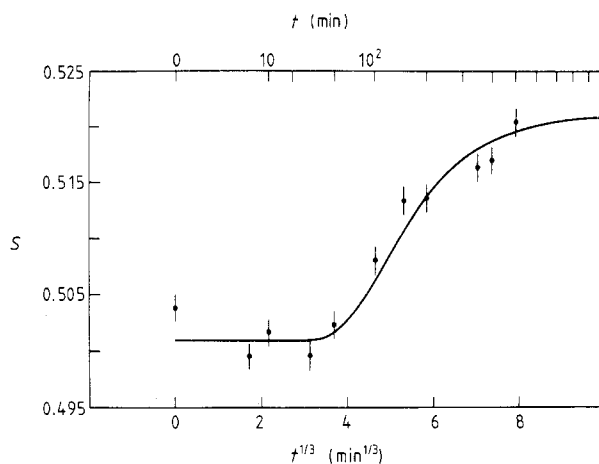


Figure 3. Doppler-broadening parameter S for positrons annihilated in the 7012 alloy versus aging time. The theoretical curve is the same as figure 2, except for the adjustment of the vertical scale.

The picture emerging from lifetime results is fully confirmed by the Doppler-broadening data reported in figure 3. these data are expressed in terms of the usual lineshape parameter S , defined as the ratio of the area of a central portion of the annihilation energy peak at 511 keV to the total area of the peak (MacKenzie *et al* 1970). Energy spectrum measurements were performed by using a pure Ge detector with an energy resolution of 1.4 keV at 477 keV; each S -point comes from the average of three spectra of ca 10^6 counts. The scattering of S -points is somewhat larger than that of lifetimes, but the substantial information on the dependence of annihilation characteristics on aging time (a monotonic increase with an initial delay of ca 50 min) is also obtained in this case, with the advantage of extremely fast data acquisition and immediate analysis procedures.

3. Discussion

We recall that the increase of positron lifetimes and the narrowing of annihilation energy peaks indicated by the increase of the S parameter, which occur for most solid materials in the presence of lattice defects even at extremely small concentrations, are due to the preferential localisation of the positron in any region of the solid where positive ions are missing or less densely packed. A positron localised in these regions has a mean life longer than in the bulk due to the local reduction of the electron density; moreover, the relative contribution of fast ion-core electrons to the overall annihilation probability is strongly suppressed, with the consequence of a reduction in the Doppler broadening of the annihilation line. The well known positron trapping model (Brandt 1967, Connors and West 1969, Bergersen and Stott 1969) translates this picture into a mathematical form, enabling us to correlate annihilation parameters with trapping rates (for applications and developments of the trapping model, see West (1973), Hautojärvi (1979) and Brandt and Dupasquier (1983)).

As already mentioned in § 1, positron trapping phenomena acting in supersaturated Al-Zn-Mg have been made clear in a series of investigations by the Halle group. In the interpretation of our results, we follow here the guidelines set by these studies; this means that we assume that the other elements present in our alloy besides Zn and Mg

do not alter the mechanism of positron trapping, even if the evolution kinetics of the alloy structure is of course affected. We also base our interpretation on generally accepted ideas on decomposition phenomena in supersaturated Al alloys (Mondolfo 1976, Löffler *et al* 1983). According to the evidence mentioned by Löffler *et al* (1983), the full decomposition sequence of Al alloys containing Zn and Mg in a ratio above 2:1 goes through the following steps starting from the homogeneous supersaturated solution obtained after quenching: (a) formation of vacancy-rich clusters (VRC) and Guinier–Preston (GP) zones; (b) transformation of GP zones in metastable semi-coherent MgZn₂ precipitates (η' phase) and, depending on the details of the aging treatment, sometimes direct nucleation of η' particles on VRC; (c) transformation of η' precipitates in stable incoherent MgZn₂ precipitates (η phase).

In our specific case, VRC have most probably disappeared from our samples before the end of the long-term room-temperature aging (Löffler *et al* 1983), and GP zones have already reached a concentration sufficient to trap almost all positrons. Inside GP zones, positrons are localised in stable vacancies associated with Mg atoms; this explains the lifetime well above the bulk Al lifetime measured after pre-aging but before the second aging step. During aging at 160 °C, the average radius of GP zones increases. At the beginning, this has no effect on annihilation parameters, because positron trapping is already saturated, and the trapped state remains unmodified; at a later stage, however, GP zones that have reached a certain critical size evolve into η' particles. From now on, average annihilation parameters are determined by the balance of the two competing processes: vacancy trapping inside surviving GP zones versus trapping in the misfit region at the incoherent boundary between η' particles and the matrix. Thus the increase of τ and S that we observe after the incubation period can be seen as the evolution from initial values τ_{GP} and S_{GP} , characteristic of the vacancy-trapped state inside GP zones, towards the limits $\tau_{\eta'}$ and $S_{\eta'}$ that would be reached for dominant trapping at η' incoherent surfaces. Further structural modifications of the alloy do not seem to occur within the time interval and at the temperature of the thermal treatment of our samples.

The above qualitative description tells us that the observed dependence of annihilation characteristics on the aging time is entirely determined by the transformation of GP zones into η' particles. Our objective now is to discuss the information on the kinetics of this process that can in fact be extracted from annihilation experimental data.

In the presence of two positron states (in our case, trapped states on GP and η' particles), the measured average parameters τ and S are given by the following equations:

$$\tau = w\tau_{\text{GP}} + (1 - w)\tau_{\eta'} \quad (1)$$

and

$$S = wS_{\text{GP}} + (1 - w)S_{\eta'} \quad (2)$$

where w and $1 - w$ are the relative occupancy probabilities of the two states. According to the trapping model, in a case of saturated trapping at two different capture centres in competition, one obtains

$$w = k_{\text{GP}}/(k_{\text{GP}} + k_{\eta'}) \quad (3)$$

where the k are trapping rates. We assume here that k_{GP} is proportional to the volume fraction occupied by GP zones that have not yet reached the critical size for the transformation into η' particles, and that $k_{\eta'}$ is, in turn, proportional to the surface extension of η' –matrix boundary. We also assume that, when a GP particle becomes an η' particle, its dimensions (characterised by an effective radius r) do not change substantially, so

that the size distribution functions for GP and η' particles join smoothly at the critical transformation radius r_c in a single function $n(r, t)$, where t is the aging time. This gives

$$k_{\text{GP}}(t) = \text{constant} \times \int_0^{r_c} r^3 n(r, t) \, dr \quad (4)$$

and

$$k_{\eta'}(t) = \text{constant} \times \int_{r_c}^{\infty} r^2 n(r, t) \, dr. \quad (5)$$

The distribution function $n(r, t)$ describes the precipitation kinetics in the alloy; it can be linked to the experimentally accessible parameters τ and S through an integral master equation obtained by combining equations (1) to (5). In a general case, this equation is not sufficient for the determination of $n(r, t)$; however, this possibility exists if the shape of $n(r, t)$ depends on t only through a scaling factor. As we show below, this can be a realistic assumption in our case.

Schematically, one can separate the precipitation kinetics of a supersaturated alloy into two stages: an initial phase characterised by the increase of the total volume of the precipitates, maintained by the excess solute present in the matrix (growth stage); and a later phase (occurring when the degree of supersaturation of the matrix has fallen close to the equilibrium level) during which the total volume of the precipitates remains constant, whereas the size of the precipitates continues to increase at the expense of their number (coalescence stage). During the growth stage, $n(r, t)$ depends on the initial conditions, i.e. on the degree of supersaturation and on the distribution of the nucleation sites, but this dependence tends to be lost in the coalescence stage. According to the LSW theory, in the latter stage the average effective radius of the precipitates $\langle r(t) \rangle$ increases in proportion to $t^{1/3}$, and $n(r, t)$ converges asymptotically to a fixed shape expressed by a relationship of the form

$$n(r, t) \, dr = N(t)p(x) \, dx \quad (6)$$

where $N(t)$ is the number of precipitates and $p(x)$ is a function of the ratio $x = r/\langle r(t) \rangle$ (for the theoretical expression of $p(x)$ see equation (10) below). By combining equations (4) to (6), one has

$$k_{\eta'}/k_{\text{GP}} = Au \int_u^{\infty} x^2 p(x) \, dx / \int_0^u x^3 p(x) \, dx \quad (7)$$

where A is a dimensionless constant and

$$u = r_c/\langle r(t) \rangle = (t/t_c)^{-1/3} \quad (8)$$

where t_c is also a constant. This is in fact the key parameter controlling the evolution of the η' phase; by taking for $\langle r(t) \rangle$ the expression given by the LSW theory, one obtains

$$t_c = 9r_c^3 k_B T / 8D\sigma v C_{\infty} \quad (9)$$

where k_B is the Boltzmann constant, T the temperature, D the diffusion constant of the solute, σ the inter-phase surface tension, v the atomic volume of the solute, and C_{∞} the concentration of the saturated solid solution. For a multi-component alloy as in the present case, one should consider 'effective' values for the above material characteristics; we shall, however, leave t_c as a parameter to be determined from a fitting to the experimental data.

In principle, one could work out a numerical solution for $p(x)$ from equation (7). However, here we do the reverse, by comparing our experimental data with the theoretical prediction which we obtain by assuming for $p(x)$ the form dictated by the LSW theory, i.e.

$$p(x) = 324x^2(3 - 2x)^{-11/3}(3 + 2x)^{-7/3}e^{-2x/(3-2x)} \quad (10)$$

and by leaving constants A and t_c in equations (7) and (8) as best-fit parameters. The result of this calculation is shown in figures 2 and 3; the curve is the same in both figures, except for the obvious adjustment of the vertical scale. The chi-squares per degree of freedom are 0.72 and 1.6, respectively, for the lifetime curve and for the S curve.

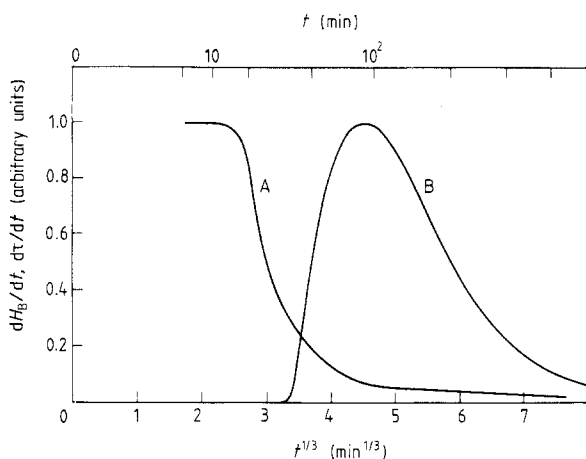


Figure 4. Derivatives of Brinell hardness and positron mean life in the 7012 alloy versus aging time. The tops of the two curves are arbitrarily normalised to 1.

The evident success of the LSW theory combined with the positron trapping model in explaining the dependence of the annihilation parameters on the aging time not only supports the interpretation scheme proposed by the Halle group, but also gives the following information on the precipitation kinetics in our alloy:

(i) The transformation of GP zones into η' particles during the second aging stage proceeds in the coalescence regime.

(ii) The size distribution of GP zones and of η' particles during this stage is adequately described by the LSW function $p(x)$.

(iii) The power law $t^{1/3}$ predicted by the theory for the mean radius increase is substantially confirmed (if one leaves the exponent of t in equation (8) as a best-fit parameter, one obtains $-1/2.7$ instead of $-1/3$).

(iv) All the variables influencing the transformation kinetics, i.e. material properties and aging temperature, control the timescale of the process through the global parameter t_c .

Point (iv) has practical implications. For instance, it indicates the possibility of predicting the incubation time for the precipitation of the η' phase in different alloys of the 7000 series and at different aging temperatures, by equation (9) and by using our experimental values $t_{\text{inc}} = 45 \pm 5$ min and $t_c = 89 \pm 5$ min (same signs of the error limits are corresponding) for evaluating the constant in the scaling rule:

$$t_{\text{inc}}/t_c = \text{const.} \quad (11)$$

As a last point, we want to remark on the lack of correlation between the hardness of the material and the precipitation of the η' phase, as detected by positron annihilation. This is evidenced in figure 4, where we have plotted the normalised derivatives of the curves in figures 1 and 2. The indication from this behaviour is that the internal stresses due to GP zones, which are sufficient to increase the hardness of the material already in the initial stage of coalescence, i.e. after the first few minutes of aging at 160 °C, are not substantially relaxed by the precipitation of the more stable η' phase.

Acknowledgments

This work was performed under a research contract ENEA/Politecnico di Milano. One of us (A Somoza) benefited from financial support by the International Centre of Theoretical Physics, Trieste, Italy, and by the Consejo Nacional de Investigaciones Científicas y Técnicas de la República Argentina.

References

- Alam A and West R N 1982 *J. Phys. F: Met. Phys.* **12** 389
 Bergersen B and Stott M J 1969 *Solid State Commun.* **7** 1203
 Bertolaccini A and Zappo L 1967 *Nuovo Cim.* **B 52** 487
 Brandt W 1967 *Positron Annihilation* ed. A T Stewart and L O Roellig (New York: Academic) p 345
 Brandt W and Dupasquier A (ed.) 1983 *Positron Solid State Physics* (Amsterdam: North-Holland)
 Connors D C and West R N 1969 *Phys. Lett. A* **30** 24
 Di Russo E and Buratti M 1979 *Metallurgia Italiana* **10** 449
 Dlubek G 1984 *Cryst. Res. Technol.* **19** 1319
 Dlubek G, Brümmer O, Hautojärvi P and Yli-Kaupilla J 1981a *Phil. Mag.* **A 44** 239
 Dlubek G, Brümmer O and Krause R 1985 *Positron Annihilation* ed. P C Jain, R M Singru and K P Gopinathan (Singapore: World Scientific) p 883
 Dlubek G, Brümmer O, Krause R, Baranowski A and Rozenfeld B 1983 *Phys. Status Solidi* **a 78** 217
 Dlubek G, Brümmer O, Yli-Kaupilla J and Hautojärvi P 1981b *J. Phys. F: Met. Phys.* **11** 2525
 Dlubek G, Kabish O, Brümmer O and Löffler H 1979 *Phys. Status Solidi* **a 55** 509
 Dlubek G, Krause R, Brümmer O and Plazaola F J 1986 *Mater. Sci.* **21** 853
 Hautojärvi P (ed.) 1979 *Positrons in Solids* Topics in Current Physics, vol. 12 (Heidelberg: Springer)
 Johnson M L, Panchanadeeswaran S, Saterlie S and Byrne J G 1977 *Phys. Status Solidi* **a 42** K175
 Kabisch O, Dlubek G, Löffler H, Brümmer O and Gerlach R 1980 *Phys. Status Solidi* **a 59** 731
 Kirkegaard P and Eldrup M 1974 *Comput. Phys. Commun.* **7** 401
 Kirkegaard P, Eldrup M, Mogensen O E and Pedersen N J 1981 *Comput. Phys. Commun.* **23** 307
 Krause R, Dlubek G and Brümmer O 1987 *Proc. Eur. Meeting on Positron Studies of Defects, Wernigerode, GDR* ed. G Dlubek, O Brümmer, G Brauer and K Hennig (Halle-Wittenberg: Martin-Luther-Universität) PL7
 Lifshitz M and Slyozov V V 1959 *Sov. Phys.-JETP* **35**
 ——— 1961 *J. Phys. Chem. Solids* **19** 35
 Löffler H, Kovács I and Lendvai J 1983 *J. Mater. Sci.* **18** 2215
 MacKenzie I K, Eady J A and Gingerich R R 1970 *Phys. Lett. A* **33** 279
 Mondolfo L F 1976 *Aluminium Alloys: Structure and Properties* (London: Butterworths) p 398
 Sedov V L, Teimurazova V A and Berndt K 1970 *Phys. Lett. A* **33** 319
 Triftshäuser W and Kögel G 1985 *Positron Annihilation* ed. P C Jain, R M Singru and K P Gopinathan (Singapore: World Scientific) p 874
 Wagner C 1961 *Z. Electrochem.* **65** 581
 Wang S and Wang Z 1982 *Positron Annihilation* ed. P C Coleman, S C Sharma and L M Diana (New York: North-Holland) p 512
 West R N 1973 *Adv. Phys.* **22** 263